EXCITABLE MEMBRANE ULTRASTRUCTURE

I. Freeze Fracture of Crayfish Axons

CAMILLO PERACCHIA

From the Department of Physiology, University of Rochester, School of Medicine and Dentistry, Rochester, New York 14642

ABSTRACT

Cross-sectioned and cross-fractured crayfish axons display regions in which axon and Schwann cell surface membranes are regularly curved and project into the axoplasm. At these regions (projections) the two membranes run precisely parallel, separated by a gap of 130–140 Å. Longitudinal fractures through the axons expose the inner fractured surface of either the internal (face A) or the external (face B) leaflet of axon and adjacent Schwann cell surface membranes. On both membranes the projections appear as elongated structures oriented with the long axis parallel to the long axis of the nerve fiber. On face A of the axon surface membrane they are seen as elongated indentations 0.5–1.2-μm long, 0.12–0.15-μm wide. The indentations contain parallel chains of globules. The chains repeat every 120–125 Å and are oriented obliquely in such a way that if one looks at the axon surface from the extracellular space, the axis of the chains is skewed counterclockwise to the long axis of the indentations by an acute angle (most often 55–60°). The globules repeat along the chain every 80–85 Å. Globules of adjacent chains are in register in such a way that the axis on which globules of neighboring chains are aligned forms an angle of 75–85° with the axis of the chains. The complex structure can be defined as a globular array with a rhomboidal unit cell of 80–85 × 120–125 Å. On face B of the axon surface membrane the complementary image of these structures is seen. The projections of the Schwann cell surface membrane also contain groupings of globules; however, these differ from those in the axonal projections in size, pattern of aggregation, and fracture properties. Several possible interpretations of the meaning of these membrane specializations could be proposed. They could be: (*a*) structures involved in the mechanism of excitation, (*b*) regions of presumed metabolic couplings, and (*c*) areas of cell-to-cell adhesion.

INTRODUCTION

The surface membranes of most nerve and muscle cells are called excitable membranes, because of their ability to initiate and conduct electrical impulses. This property (excitability) is the consequence of voltage-dependent changes in sodium and potassium conductances across the membrane (16). The most widely accepted hypothesis attributes the conductance changes to the sudden opening of hydrophilic channels existing in the membrane, to provide selective ionic pathways between the cytoplasmic and the extracellular environment (18, as review).

Unusual structures may be present in excitable membranes to account for the peculiarity of their function and may be detectable by morphological methods. This hypothesis has stimulated the present series of studies, whose primary aim is to provide a detailed description of the freeze-fracture appearance of excitable membranes.

By conventional ultrastructural methods, axon surface membranes usually display, in cross section, a typical trilaminar profile ~85-Å thick. In squid giant axon the internal electron-opaque layer has been reported (41, 43) to be slightly thicker than the external and to occasionally display local areas of thickening, interpreted (42) as sites of active transport, in correspondence with narrowing of the extracellular space between axon and satellite cell. In addition the existence of membrane regions containing a presumed globular structure has been suggested in axon and Schwann cell surface membrane (41, 43). This suggestion, however, was based only on sectioned material, while it is now generally agreed that freeze fracture is the only morphological method that gives meaningful data on globular structures in membranes.

In crayfish nerve cords the osmiophilia of axon surface membranes has been found to increase as a result of electrical stimulation, asphyxia, or treatment with reducing agents (26). The change in osmiophilia also occurred in endoplasmic reticulum and outer mitochondrial membranes but never in inner mitochondrial and Schwann cell membranes. The phenomenon has been interpreted as due to the presence of sulfur-rich proteins in which SH groups would be unmasked as a result of the various treatments and would consequently react with osmium.

Only a few freeze-fracture studies have been performed on nerve excitable membranes. Freeze fractures through the axon surface membrane of an insect photoreceptor cell exposed protrusions (subunits) arranged in regular arrays with a unit cell dimension of 115 × 150 Å (12). The arrays are interspaced by relatively smooth regions. Arrays of this kind have not been reported in recent freeze-fracture studies of axon surface membranes in mammalian nerves (8, 9), although peculiar aggregations of globules have been described (8).

Several experiments have been performed on the isolation and biochemical characterization of excitable membranes. In squid giant axons two membrane fractions of different density have been isolated (5). The less dense fraction, interpreted as composed mainly of axon surface membranes, has a high content of Na^+-K^+-dependent, ouabain-sensitive ATPase, in agreement with the high ATPase activity detected histochemically in surface membranes of intact axons (31). More recently, very pure fractions of axon surface membranes have been isolated from squid retinal axons (11). These membranes display also a high specific activity of ouabain-sensitive ATPase, and are composed of highly unsaturated phospholipids (45).

The present study describes several peculiar structures observed in crayfish axon and Schwann cell surface membranes. Particular emphasis is given to the structural features and possible functional meaning of regularly repeating chains of globules which are present only in the axon surface membranes.

FIGURE 1 Cross-sectioned axon of medium size (~20 μm in diameter). In certain regions the two adjacent axon and Schwann cell surface membranes project towards the axoplasm. These projections (arrows) repeat every 1–3 μm. The axoplasm is packed with microtubules. The microtubules at the center of the axon are cross sectioned, while most of the others are obliquely sectioned and seem to swirl around the center of the axon. × 5,500.

FIGURE 2 Cross section through the wall of a medium-size axon. At the projections (arrows), axon and Schwann cell surface membranes are regularly curved and run precisely parallel, separated by a gap of 130–140 Å. The projections are not associated with cytoplasmic organelles either in the axon or in the Schwann cell (*S*). *Ax*, axoplasm; *C*, connective tissue. × 26,000.

FIGURE 3 Cross fracture through the wall of a large-size axon. The course of the axon-Schwann cell surface membranes is less tortuous than in sections, probably because of less extensive shrinkage of freeze-fractured specimens. For the same reason, the projections (arrows) do not extend as deeply into the axoplasm. *Ax*, axoplasm; *S*, Schwann cell. × 26,000.

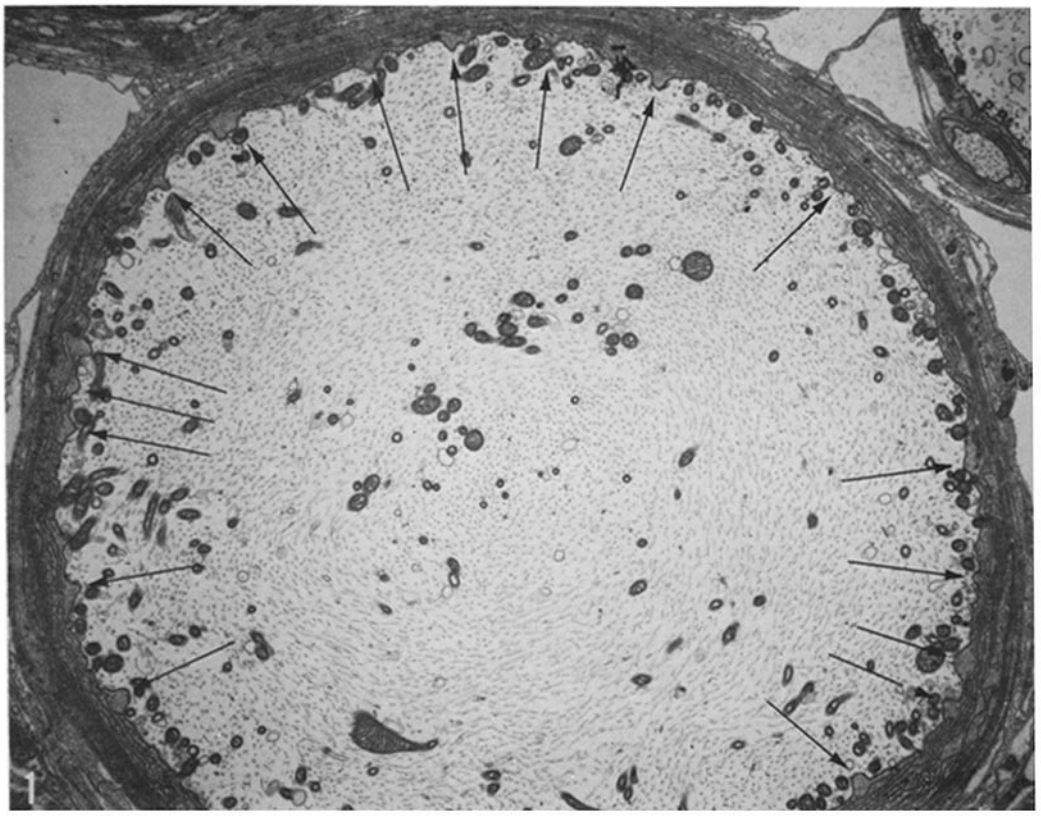

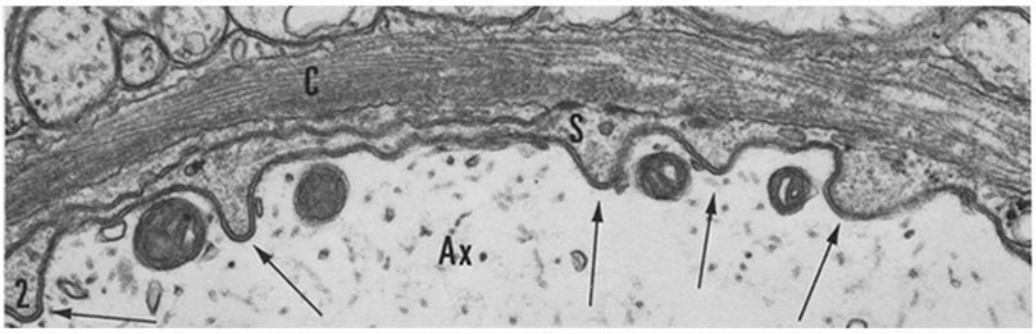
C
S
Ax

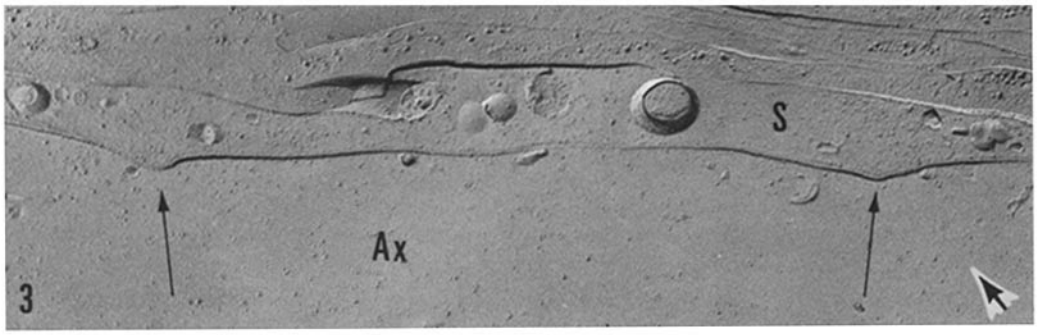
S
Ax

MATERIALS AND METHODS

Sections

Crayfish (*Procambarus clarkii*) were sacrificed by decapitation. 3–6% glutaraldehyde-H_2O_2 (25) buffered to pH 7.4 with 0.1 M (Na, K) phosphate was injected into the abdomen at room temperature. A few minutes later the abdominal nerve cord was dissected out of the animal and kept in the same fixative for 2 h. After a 30-min wash in 0.1 M phosphate, the cord was postfixed for 2 h at room temperature in 2% OsO_4, buffered to pH 7.4 with phosphate. Dehydration was carried out in graded alcohol and embedding in Epon. Thin sections were cut with an LKB Ultrotome microtome and stained for 15 min by immersion in a saturated solution of uranyl acetate in 50% ethanol, followed by a 3-min immersion in a 3% solution of lead salts (32).

Freeze Fracture

Abdominal nerve cords, fixed for 1 h in glutaraldehyde-H_2O_2, were immersed in a 5, 10, 20, 30% series of glycerol solutions at 30-min to 1-h intervals at 4°C. Interganglionic portions of the nerve cords were cut into segments ~1-mm long and mounted on aluminum holders. The specimens were rapidly frozen in liquid Freon 22 (Virginia Chemicals Inc., Portsmouth, Va.) at ~−150°C and transferred to a Denton freeze-fracture device (Denton Vacuum Inc., Cherry Hill, N. J.) mounted on a Kinney (KSE-2A-M) evaporator (Kinney Vacuum Co., Boston, Mass.). The shroud and the specimen holder were previously cooled with liquid nitrogen. The segments of nerve cord were fractured longitudinally at ~−110°C and immediately shadowed with carbon-platinum at 45° followed by carbon at 90°. All the replicas were performed at a vacuum of approximately 2×10^{-7} torr. Dry nitrogen was introduced into the bell jar and the replicas were immediately coated with a drop of 2% collodion in amyl acetate (S. Bullivant, and R. S. Weinstein, 1972, personal communication). As soon as a collodion film formed on the surface of the replicas, the specimens were digested in Chlorox and the collodion-coated replicas, washed three times in distilled water, were collected on uncoated 400-mesh grids. The collodion film was then dissolved by immersion of the replicas in amyl acetate for 2–3 min. The collodion coating strengthens the replica during tissue digestion, allowing one to recover even large replicas undamaged. All specimens were examined with an AEI EM 801 electron microscope. The microscope magnification was standardized before each photographic exposure by eliminating the hysteresis of the lenses. All magnification steps were previously standardized with a carbon grating replica (no. 1002, Ernest Fullam, Inc., Schenectady, N. Y.). The black and white arrow, in freeze-fracture micrographs, indicates the direction of platinum shadowing.

OBSERVATIONS

Crayfish nerve fibers, transversely sectioned, display the profiles of the axon and the adjacent Schwann cell surface membranes, running roughly parallel, separated by a narrow gap. In certain regions the two membranes are regularly curved and run precisely parallel, separated by a gap of 130–140 Å, projecting to a certain extent into the axoplasm (Figs. 1, 2). These projections repeat, in large axons, every few micrometers and do not seem to be specifically associated with axoplasmic organelles. At the projections the cytoplasm of the Schwann cell contains the same finely granular or filamentous material seen elsewhere in the cell (Fig. 2), but never mitochondria, and membranes of the endoplasmic reticulum or the tubular lattice (17, 26, 27). The projections are more frequent in medium- and large-size axons than in small axons.

In freeze-fractured preparations the course of cross-fractured axon-Schwann cell surface membranes is fairly straight (Fig. 3). The projections are visible but do not extend into the axoplasm as deeply as in sections. Fractures tangential to the axon surface expose the inner fractured face of either the internal (face A) or the external (face B) leaflet of the axon and its adjacent Schwann cell surface membranes. On both membranes the projections appear as elongated structures oriented with the long axis parallel to the long axis of the nerve fiber. On the axon surface membrane, face A (AFA), they are seen as elongated indentations (Figs. 4–6,11). The indentations are randomly distributed and measure 0.5–1.2 μm in length and 0.12–0.15 μm in width. Most of them have an ellipsoidal shape with the long axis straight or just slightly bent, some are composed of two or three segments; others are shaped as a Y (Fig. 5). Frequently the indentations bend sharply to the right or to the left at an angle of 125–135°.

Viewed at higher magnification the indentations contain parallel chains of globules (Fig. 6). The chains repeat at a periodicity of 120–125 Å and are obliquely oriented in such a way that if one looks at the axon surface from the extracellular space, the long axis b of the chains is skewed counterclockwise with respect to the long axis a of the indentations by an acute angle (Figs. 6, 8). This angle most frequently measures 55–60° but

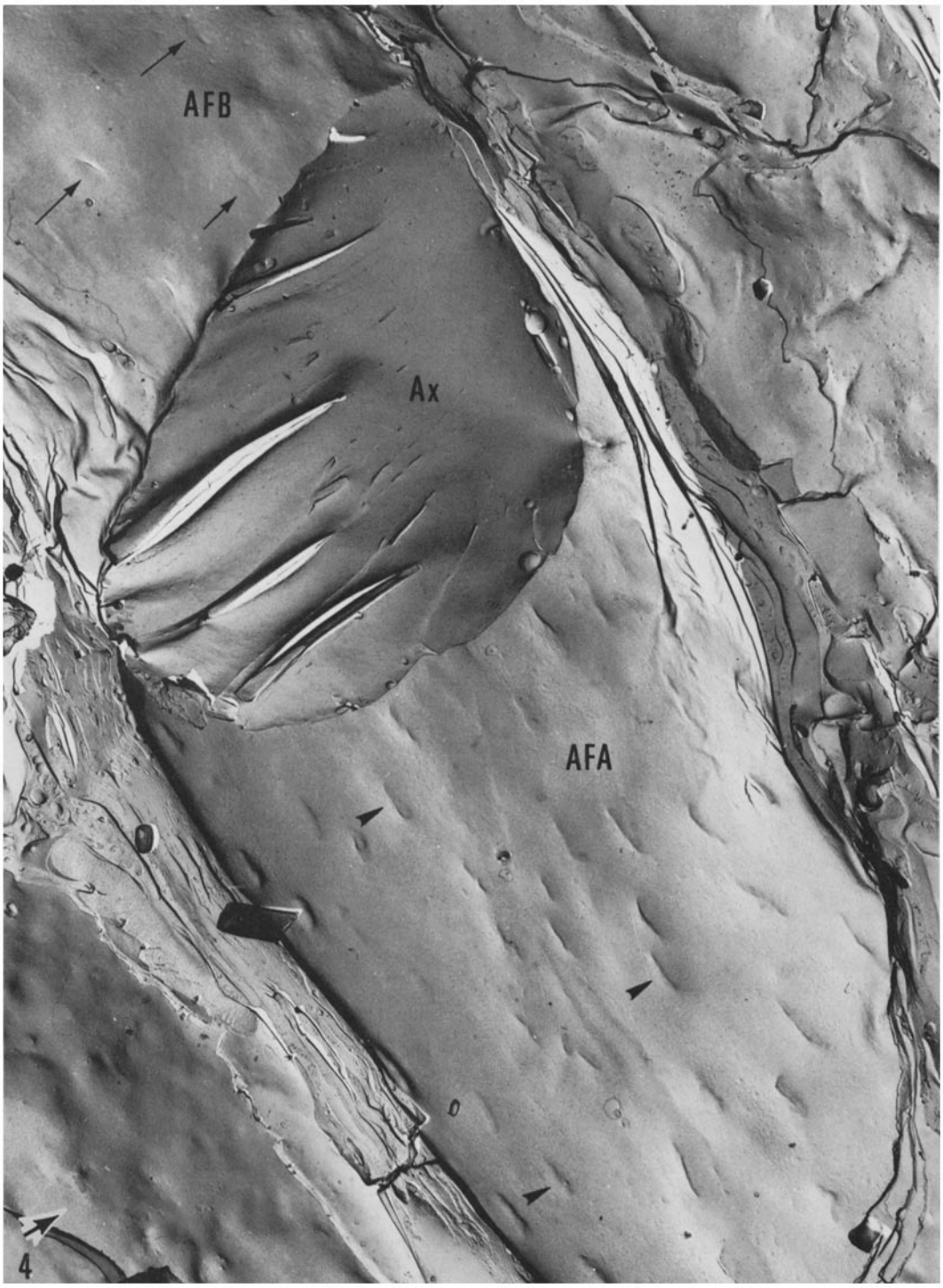

FIGURE 4 Medium-size axon, obliquely fractured. A large area of the axon surface, face A (*AFA*) is exposed. Here the projections appear as elongated, randomly distributed indentations (arrowheads), all oriented with the long axis parallel to the long axis of the fiber. Elongated protrusions (arrows), complementary images of the indentations, are faintly visible on axon surface, face B (*AFB*). *Ax*, axoplasm. × 7,500.

ranges from 43 to 75° (Fig. 9). The globules measure ~80 Å and repeat along the axis of the chains at a center-to-center distance of 80–85 Å. The globules of one chain are in register with those of the adjacent chain and are aligned along an axis c which lies at an angle of 75–85° (most frequently ~80°) with the axis b of the chains (Figs. 6, 8). Preliminary observations suggest that globular arrays with the widest angles between axis a and b display the narrowest angles between axis b and c, and vice versa. The complex structure can be defined as a globular array with a rhomboidal unit cell of 80–85 × 120–125 Å (Fig. 8).

Indentations 1-μm long contain ~1,000 globules. If plotted to the total membrane surface, the number of the globules, in large axons, is 200–400/μm^2 of axon surface membrane. Apart from these structures, the axon's face A does not show unusual characteristics, appearing as a relatively smooth surface, studded with randomly distributed globules, 60–110 Å in size, numbering ~1,500/μm^2 of membrane surface (Fig. 5, inset; Figs. 6, 11), and, less frequently, pits (Fig. 6).

On the axon surface membrane, face B (AFB), elongated protrusions are seen, representing the complementary images of the indentations (Figs. 4, 7, 10). At high magnification the protrusions appear furrowed by parallel, obliquely oriented grooves which repeat at a periodicity of 120–125 Å (Figs. 7, 10). The axis of the grooves (axis b) is skewed clockwise with respect to the longitudinal axis of the protrusions (axis a), by an acute angle. As for the indentations, this angle most often measures 55–60° ranging from 43 to 75°. Frequently the long axis of the protrusions is bent by an angle of 125–135° (Fig. 10). The grooves are visible along the entire surface of the bent protrusions, but the orientation of their axis changes abruptly in the bends (Fig. 10, inset).

Due to contamination, in most replicas only the appearance of parallel grooves is detectable on the protrusions (Fig. 10). Replicas of higher resolution, however, show that the grooves are formed by chains of pits (Fig. 7), which represent the complementary images of the chains of globules (Fig. 6). As expected, pits of neighboring chains are aligned in rows whose axis c forms an angle of 75–85° with the axis b of the chains.

Between protrusions, the axon surface membrane, face B, does not display peculiar characteristics. Few globules 60–110 Å in size (Figs. 7, 10) and numerous pits (Fig. 7) are randomly distributed on a relatively smooth surface. The globules number 200–300/μm^2 of membrane surface.

As seen in cross-sectioned (Figs. 1, 2) and cross-fractured (Fig. 3) axons, the surface membrane of the Schwann cell closely follows the course of the axon surface membrane at the projections. Consequently protrusions and indentations are expected on the Schwann cell surface membrane face A (SFA) and B (SFB), respectively. Face A displays protrusions (Figs. 10, 12) similar in size and shape to the ones seen in the axon membrane. Schwann cell protrusions contain several globules 100–110 Å in size, and more rarely pits, irregularly distributed on a rather smooth surface (Fig. 12). Although globules of similar size can also be seen in membrane regions between protrusions, the density of this size globule at the protrusions is greater than elsewhere. Some of these globules display a central electron-dense dot, possibly a depression.

Membrane regions between protrusions (Figs. 10, 12) contain many scattered globules and a few pits (Fig. 12) whose size range, number, and distribution correspond to those of the globules and the pits located between the indentations on face

FIGURE 5 Tangential fracture along the surface membrane of a large axon. The fractured surface of the internal membrane leaflet (face A) (*AFA*) is exposed. Numerous elongated indentations (arrowheads) are seen. Most are ellipsoid shaped with the long axis straight or slightly bent. Some are composed of two or three segments, others are shaped as a Y. The *inset* enlargement shows a portion of axon surface membrane, face A (*AFA*), partially covered by a sheetlike Schwann cell process (*Sc*, Schwann cell cytoplasm). Regions of *AFA* between indentations contain random globules (~1,500/μm^2), 60–110 Å in size. The Schwann cell process is overlapped by the surface membrane (face B) (*SFB*) of an adjacent Schwann cell. This membrane displays several small gap junctions (face B) (arrows) and random, conical protrusions (small arrowheads). The gap junctions are regions of presumed coupling between the adjacent Schwann cells. The conical protrusions are surface membrane invaginations which form the tubular lattice. × 8,500; *Inset*, × 23,000.

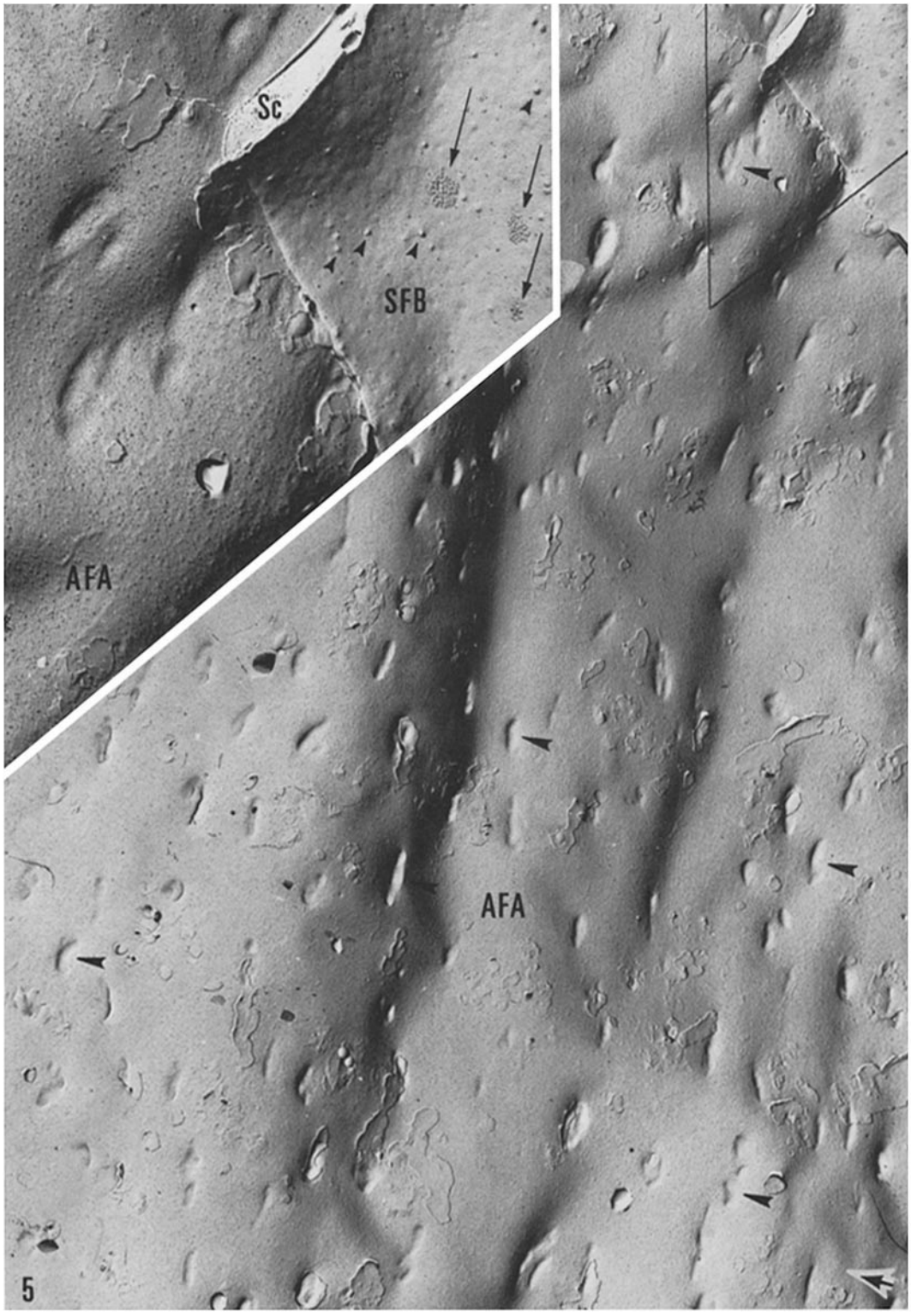
Sc
SFB
AFA
AFA
5

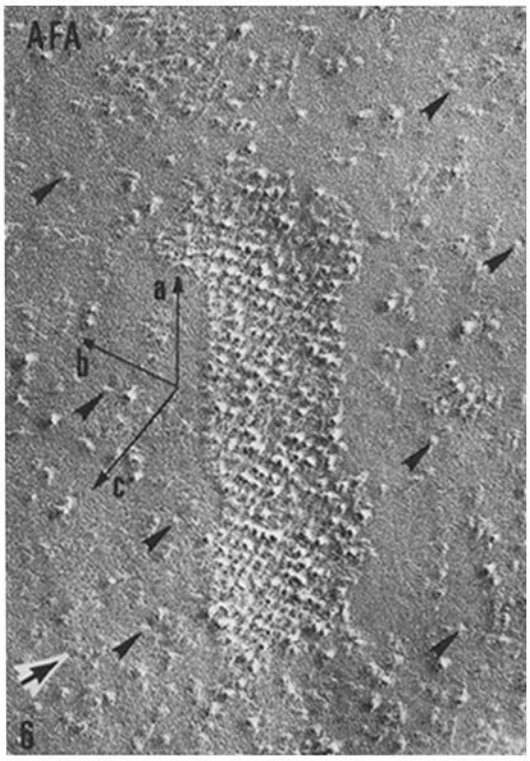

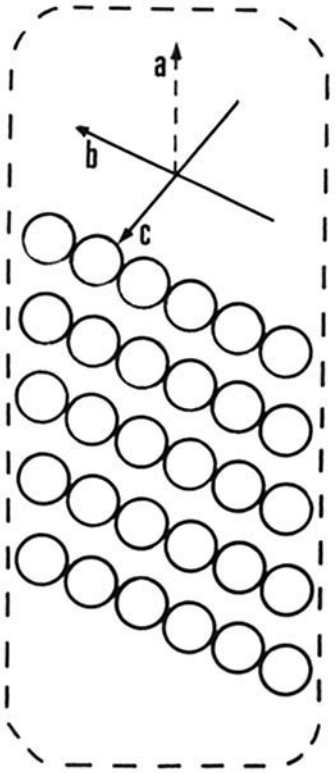

8

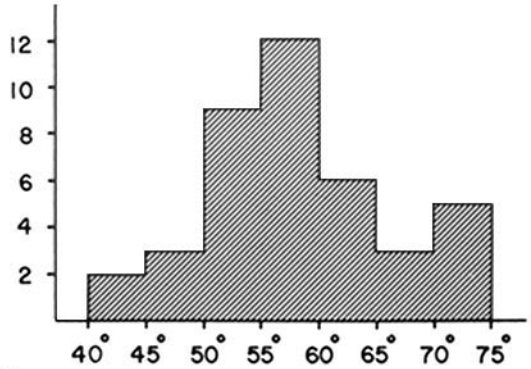

9

A of the axon surface membrane. In addition Schwann cell's face A displays several circular dimples ~400 Å in diameter (Figs. 10, 12), representing the mouth of tubular invaginations of the surface membrane which form the tubular lattice (17, 26, 27).

On face B of the Schwann cell surface membrane, elongated indentations are seen containing numerous globules 100–110 Å in size (Figs. 11, 13). Frequently these globules display some regularity in their aggregation, being aligned in rows slightly skewed to the long axis of the indentation (Fig. 11, inset). Rarely pits are also seen between the globules (Fig. 13), indicating that some of the globules are cleaved away together with the internal membrane leaflet. Membrane regions between indentations contain few globules, 60–110 Å in size (Figs. 11, 13), and numerous pits (Fig. 13). These regions are not obviously different from the regions between protrusions on face B of the axon surface membrane. In addition Schwann cell's face B shows conical protrusions ~400 Å in diameter (Fig. 5, inset; Fig. 11, inset; Fig. 13) which represent the complementary images of the dimples previously described (Figs. 10, 12). Frequently these protrusions display a raised circular rim limiting a central depression (Fig. 11, inset; Fig. 13). The rim represents the cross-fracture profile of the invaginating membrane tubule. The central depression corresponds to the lumen of the tubule.

Regions of Schwann cell surface membrane not adjacent to the axon surface membrane do not display projections and structural specializations similar to those seen at the projections, but frequently contain gap junctional specializations (Fig. 5, inset). The diagrams in Fig. 14 show an interpretation of the profile of axon and Schwann cell membrane specializations at the projections, before (Fig. 14 *a*) and after (Fig. 14 *b*) fracture.

DISCUSSION

This study has produced evidence that excitable membranes of crayfish axons contain well-defined structures with unusual features. These structures are composed of chains of globules which repeat at a precise periodicity forming regular arrays with a rhomboidal unit cell. Regions of Schwann cell surface membranes adjacent to these arrays also display groupings of globules. These globules, however, differ from those of the rhomboidal arrays in size, pattern of aggregation, and fracture properties. In both cells the specializations are associated with elongated membrane projections oriented parallel to the long axis of the axon.

The observation of regular arrays of globules is not unusual in membranes. In most cases closely packed globules form fairly regular hexagonal arrays. These arrays occur most often where the plasma membranes of two adjacent cells come in

---

FIGURE 6 Globular arrangement at an indentation of the axon surface membrane (face A) (*AFA*). Globules ~80 Å in size are aligned in parallel chains which repeat at a periodicity of 120–125 Å. The center-to-center distance between adjacent globules along a chain is 80–85 Å. The longitudinal axis b of the chains is skewed counterclockwise with respect to the long axis a of the indentation by an acute angle of variable size (see histogram, Fig. 9). Globules of neighboring chains are in register and are aligned along an axis c, which forms an angle of 75–85° with the long axis b of the chains. Outside the indentation, *AFA* displays many random globules, 60–100 Å in size, and few pits (arrowheads). × 150,000.

FIGURE 7 Elongated protrusion on the axon surface membrane (face B) (*AFB*). The protrusion displays oblique grooves, oriented along axis b. The grooves are composed of chains of pits (complementary images of the chains of globules). As in the case of the globules (Fig. 6), pits of neighboring grooves are in register and are aligned along an axis c which forms an angle of 75–85° with the axis of the grooves. The alignment of the pits along axis c is seen more clearly if the micrograph is bent sharply and observed along the direction of axis c. Membrane regions outside the protrusions display a few globules 60–110 Å in size and some pits (arrowheads). × 150,000.

FIGURE 8 Schematic diagram of the chain arrangement of the axonal globules viewed from the extracellular space. The globules of neighboring chains are in register, forming a pattern with a rhomboidal unit cell of 80–85 × 120–125 Å. The angles between the three axes of the pattern vary; the angle between axis a and b measures 43–75° (most often 55–60°) (see histogram, Fig. 9). The angle between b and c measures 75–85°.

FIGURE 9 Histogram of the frequency of various size angles between axis a and b (see Fig. 8).

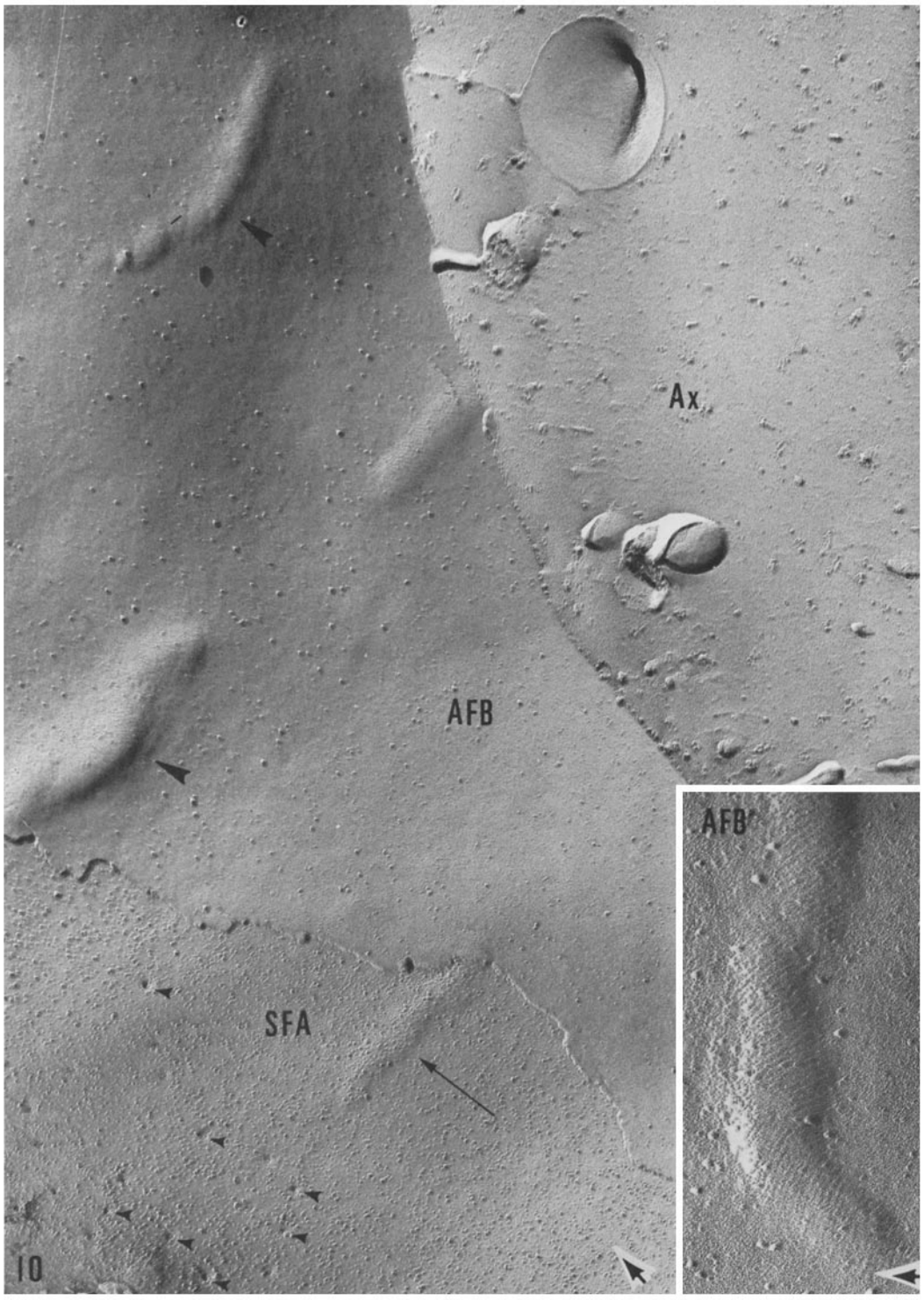
Ax
AFB
AFB'
SFA
10

close apposition to form gap junctions (21, as review). In one case, hexagonal arrays have also been reported in a nonjunctional membrane, the plasma membrane of epithelial cells in mammalian urinary bladder (6, 14, 37, 40).

Square arrays of globules also occur but less frequently than the hexagonal ones. First reported in sectioned plasma membranes of intestinal epithelial cells of suckling rat (44), similar, but smaller, arrays were recently found in freeze fracture of the same membranes in adult rat (36). The interpretation (36) of these arrays as components of an unusual type of gap junction is unlikely in light of recent observations of the same structures in surface membranes of most vertebrate skeletal muscles (C. Franzini-Armstrong, 1973, personal communication).

Regular arrays of globules with a rhomboidal unit cell rarely occur. One could be the regular lattice with a unit cell of 115 × 150 Å described in surface membranes of an insect photoreceptor (12). Judging from the only micrograph available, this pattern seems to have a rhomboidal unit cell and could be basically similar to the one described in the present study although differing in globule size and unit cell dimensions. In any event the arrays seen in crayfish and insect axon surface membranes display the common feature of being composed of parallel and regularly repeating chains of globules. This observation, together with the fact that both occur in excitable membranes, suggests that they may also have a similar functional meaning.

The globules forming the rhomboidal array are closely packed along the axis of the chains but are separated from those of adjacent chains by an edge-to-edge distance of at least 40 Å. This suggests that the globules could be in direct contact with each other along the chain, while other components may be interspaced between opposite globules of neighboring chains. If these components were lipids in a bilayer, one would expect only a few molecules per monolayer to fit between two adjacent globules, since the cross-sectional area of lipid molecules is 40–43 $Å^2$ in the gel and 60–70 $Å^2$ in the mesophase state (13, 35).

The existence of separations between globules arranged in a regular pattern is not a common feature. More frequently, in fact, the globules forming regular arrays are closely packed, suggesting that they may be directly in contact with each other and somehow linked together. On two occasions, however, hexagonal arrays were reported in which the globules are not closely packed, but are separated by an edge-to-edge distance of 75–100 Å (23, 24, 36). The hypothesis (24) that here a few lipids in a bilayer may separate the adjacent globules was suggested by the observation that the smooth fractured surface between adjacent globules (or pits in the complementary surface) is continuous, without a step, with the smooth surface of nonjunctional membrane regions which is generally agreed (4, 7, 29, 38) to correspond to the central plane of the lipid bilayer.

The possibility that the array of globules varies is suggested by the range of angles reported between the axes of the pattern. The variations in the orientation of the axes could result from distortions; however, the possibility that they represent meaningful changes in the aggregations of the components of the pattern should be taken into consideration. Potentially interesting in this regard is the observation that a decrease in the size of the angle between axis a and b seems to coincide with an increase in the angle between axis b and c. This could result from a limited sliding of each

FIGURE 10 Oblique fracture through a large axon. The fracture plane steps from the axoplasm (*Ax*) to the axon surface membrane (face B) (*AFB*) and then to the Schwann cell surface membrane (face A) (*SFA*). On *AFB* the projections are seen as elongated protrusions (complementary image of the indentations seen on AFA). At higher magnification (*inset*) the protrusions appear furrowed by parallel, oblique grooves, which repeat every 120–125 Å. The long axis of the protrusion shown in the *inset* is bent sharply by an angle of ~135°. Bent protrusions are also seen in the main micrograph (large arrowheads). Between protrusions, *AFB* displays random globules (200–300/μm^2), 60–110 Å in size. The projections of the Schwann cell surface membrane appear, on face A (*SFA*), as elongated protrusions (arrow). *SFA* is frequently studded with circular dimples (small arrowheads) ~400 Å in diameter. The dimples are the mouth of tubular invaginations of the surface membrane which form the tubular lattice and are the complementary image of the conical structures seen in Fig. 5 (*inset*). × 53,000; *inset*, × 98,000.

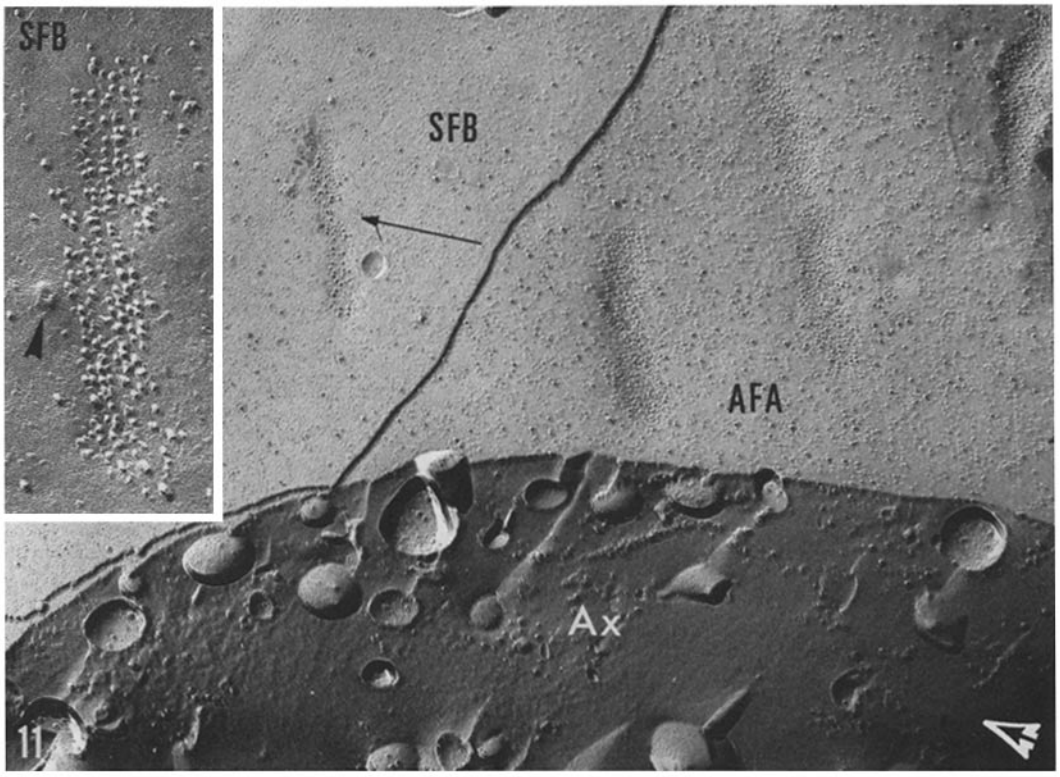
SFB
SFB
AFA
Ax
11


SFA
12


SFB
13

chain of globules along the axis of the chain itself and could reflect changes in the spatial relationship among the components of the globules.

The various shapes of the projections such as Y images, bendings, segmentations etc., may result from the confluence and fusion between two or more ellipsoidal projections. This interpretation is supported by the fact that, in bent projections, the orientation of the oblique chains of globules or pits changes abruptly at the bends, but the angle between the chains and the long axis of the corresponding segment of projection does not change.

The size of the angle at which the projections are bent has a limited range of variation (125–135°), suggesting that it may reflect certain crystallographic features of the rhomboidal pattern. The paracrystalline structure of the pattern may also condition the curved shape of the membrane at the projections.

The globular aggregates associated with the Schwann cell projections differ in several aspects from the rhomboidal arrays. The Schwann cell globules are larger, fracture occurs on either the cytoplasmic or the extracellular side, and they are not organized as regularly as the axonal globules.

The observation that all the axonal globules (at the projections) fracture away with the internal membrane leaflet suggests that they are bound more firmly to the internal than to the external leaflet, perhaps because they are asymmetrically placed with respect to the splitting plane of the membrane. On the other hand, the alternate fracture properties of the Schwann cell globules at the projections indicate a more symmetrical binding strength between the globules and either one of the membrane leaflets. The fact that the Schwann cell globules associated with the projections frequently display some regularity in their aggregation suggests that they may form a regular pattern which is distorted during the freeze-fracture procedure.

Several possible interpretations of the meaning of these membrane specializations could be discussed. (*a*) They could be structures directly involved in the excitation mechanism, each of the axonal globules possibly representing the framework of Na^+ and/or K^+ channels of excitability. (*b*) They could be regions where presumed metabolic or other type couplings between Schwann cell and axon take place. (*c*) They could be areas of cell-to-cell adhesion.

It is now generally agreed that excitability in nerve depends on the sudden changes in the permeability properties of selective channels for Na^+ and K^+ across the surface membrane (18, as review). Could these channels be seen directly by freeze fracture? At present the limiting resolution of this technique (~25 Å) excludes the possibility

FIGURE 11 Oblique fracture through a medium-size axon. The fracture plane steps from Schwann cell surface membrane, face B (*SFB*), to the axon surface membrane, face A (*AFA*), and then to the axoplasm (*Ax*). On *SFB* the Schwann cell projections appear as elongated indentations (arrow). The indentations contain groupings of globules uniform in size (~100 Å). These globules are not clearly arranged in a regular pattern; frequently, however, they seem to be aligned in rows (*inset*). The arrowhead in the *inset* points to a conical protrusion representing an invagination of the surface membrane to form the tubular lattice. × 24,000; *inset*, × 98,000.

FIGURE 12 Schwann cell surface membrane, face A (*SFA*). An elongated protrusion (on the left half of the micrograph) displays several globules 100–110 Å in size, and more rarely pits (arrows), distributed at random. Occasionally the globules show a central electron-opaque dot, possibly a depression. Membrane regions between protrusions (right half of micrograph) contain scattered globules, and few pits (arrows), 60–110 Å in size. The density of 100–110 Å globules is much greater at the protrusions than elsewhere. The arrowheads point to circular dimples ~400 Å in diameter which correspond to membrane invaginations forming the tubular lattice. × 95,000.

FIGURE 13 Schwann cell surface membrane, face B (SFB). An elongated indentation (on the right half of the micrograph) contains many 100–110 Å globules and some pits (arrows) irregularly grouped. The membrane regions between indentations display few 60–110 Å globules and many pits (arrows) randomly distributed, showing good complementarity with comparable *SFA* regions (Fig. 12). The arrowheads point to conical protrusions which display a raised circular rim limiting a central pit. These protrusions correspond to the invaginating tubules of the tubular lattice. The rim represents a cross fracture through the extracellular leaflet of the tubular membrane and the central pit, the lumen of the tubule. × 95,000.

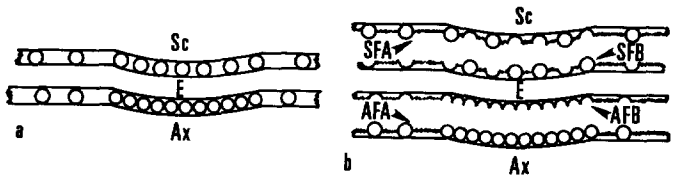

FIGURE 14 Schematic diagram of an interpretation of the profile of axon and Schwann cell surface membranes at the projections, as before (Fig. 14 *a*) and after (Fig. 14 *b*) fracture. The axon membrane contains chains of ~80-Å globules. The globules are sectioned here along the axis of the chain. The Schwann cell membrane contains globules ~100 Å in size. During freeze fracture the membranes split. All the axonal globules in chains remain attached to the internal membrane leaflet, appearing as bumps on face A (*AFA*). Face B (*AFB*) shows grooves formed by chains of pits (complementary image of the chains of globules). Of the Schwann cell globules located at the projection, some remain attached to the internal membrane leaflet (*SFA*), others to the external (*SFB*). *Ax*, axoplasm; *E*, extracellular space; *Sc*, Schwann cell cytoplasm.

of resolving structures as small as these channels. Na^+ channels are presumed, in fact, to be 3 × 5 Å in cross section (15) and K^+ channels may be even narrower (3).

It is obvious, however, that hydrophilic channels in membranes must be supported by some sort of a macromolecular framework, which would necessarily be much larger than the channels themselves and could be visible in freeze fracture of membranes.

In general, direct morphological evidence of ionic channels in membranes is not available; however, the possibility that certain ionic pathways are associated with some of the globules which become exposed in fractured membranes has been suggested on several occasions. One of these is the case of low resistance junctions. These junctions provide direct intercellular communication by means of hydrophilic pathways for ions and other molecules up to at least 1,000 mol wt (20). Morphologically the junctions correspond to regions of cell-to-cell contact (gap junctions), in which each of the two adjacent surface membranes contains hexagonally packed globules (21, as review). In certain low resistance junctions (23, 24) the globules have been seen to occupy the entire thickness of the membrane protruding from both membrane surfaces, and to be composed of six main subunits radially distributed around a central depression on either the cytoplasmic or the extracellular end. These depressions have been tentatively interpreted (24) to represent, respectively, the intracellular and the extracellular mouth of the channel. These data, together with the increasing evidence for the proteinaceous nature of membrane globules (30, 39), suggest that the framework of ionic channels could be represented by multiple subunit globular proteins spanning the membrane thickness.

A recent freeze-etch study on red cell ghosts (28) could be in agreement with this view. Here a deep etching produced a collapse of the membrane surface only at those regions which contained groupings of globules, suggesting that the water which sublimed from the bulk of the ice located beneath the membrane may have escaped mainly through the globular regions. However, alternative explanations for this phenomenon not involving membrane globules cannot yet be ruled out.

On the basis of these considerations it is reasonable to believe that the channels of excitability are also likely to be associated with some of the membrane globules. The number of these channels is still uncertain. Using the specific binding capacity of tetrodotoxin (TTX) to Na^+ channels (19, 22), it has been reported that 1 μm^2 of axon surface membrane contains no more than 75 Na^+ sites in rabbit vagus, 45 in crab nerve, and 36 in lobster nerve (walking leg) (19). Similar values are given for the K^+ channels (67 K^+ channels/μm^2 in squid giant axons) (1).

1 μm^2 of crayfish axon surface membranes of medium- and large-size axons contains 200–400 globules in rhomboidal arrays and 1,700–1,800 randomly distributed (sum of the random globules on both fractured faces). The channels of excitability could be associated with globules of either of the two groups. However, it is interesting that the globules forming the rhomboidal arrays are a peculiar feature of the axon membrane only, while the random globules occur with parallel features also in the unexcitable Schwann cell surface membrane. On the other hand, it may be surprising to learn that the channels of excitability are grouped

in discrete membrane regions, since group arrangements may result in excessive K^+ accumulation and Na^+ depletion effects during activity.

Regarding the hypothesis that the structures here described represent the morphological correlates of a metabolic coupling between axon and Schwann cell, it should be emphasized, first of all, that the evidence for such a coupling is still circumstantial. Some evidence for the possible migration of molecules from the Schwann cell to the axon (33, 34) and vice versa (2) has recently been obtained in normal and transected nerves treated by labeled amino acids or RNA precursors.

Assuming that the projections are regions where the presumed metabolic coupling takes place, it is clear that such a coupling would not occur by direct exchange of material between the two cell cytoplasms, as between cells coupled by low resistance junctions. The projections, in fact, differ from gap junctions in several features, as previously mentioned, and there is no evidence that the two cells are electrically coupled. A possible mechanism could be a two-step migration in which the material to be transferred between the two cells would at first be transported into the extracellular space and then be taken up by the adjacent cell.

Whether or not the projections represent areas of cell-to-cell adhesion, little can be discussed at present. It is generally agreed that desmosomes are the prominent structures of cell-to-cell adhesion. Desmosomes, however, differ from the structures here described, being formed by two symmetrical membranes which display, in freeze fracture, closely packed granules and short filaments on both fracture faces (21). In any event, the possibility that the projections represent an unusual type of cell-to-cell adhesion should be kept in mind.

The observations presented here indicate that excitable membranes of crayfish axons contain unusual specializations which are closely associated with different specializations of the Schwann cell surface membrane. The axonal structures are composed of parallel, periodically repeating chains of globules which form a regular array with a rhomboidal unit cell. The Schwann cell structures are formed by grouping of globules which are larger and less regularly arranged than those of the axon. The significance of these structures is still hypothetical and various possibilities including involvement in the excitation mechanism, in Schwann cell-axon metabolic coupling, and in cell-to-cell adhesion should be tested.

The author wishes to thank Mrs. Lillian Peracchia for her technical assistance and for the preparation of the diagrams.

This research was supported by a grant from the National Institutes of Health (1 PO1 NS 10981-01).

Received for publication 16 July 1973, and in revised form 15 October 1973.

REFERENCES

1. Armstrong, C. M. 1966. *J. Gen. Physiol.* **50**:491.
2. Autilio-Gambetti, L., P. Gambetti, and B. Shafer. 1973. *Brain Res.* **53**:387.
3. Bezanilla, F., and C. M. Armstrong. 1972. *J. Gen. Physiol.* **60**:588.
4. Branton, D. 1966. *Proc. Natl. Acad. Sci. U. S. A.* **55**:1048.
5. Camejo, G., G. M. Villegas, F. V. Barnola, and R. Villegas. 1969. *Biochim. Biophys. Acta.* **193**:247.
6. Chlapowski, F. J., M. A. Bonneville, and L. A. Staehelin. 1972. *J. Cell Biol.* **53**:92.
7. Deamer, D. W., and D. Branton. 1967. *Science (Wash. D. C.).* **158**:655.
8. Dermietzel, R., and H. Brettschneider. 1973. *Z. Zellforsch. Mikrosk. Anat.* **137**:111.
9. Devine, C. E., F. O. Simpson, and W. S. Bertand. 1971. *J. Cell Sci.* **9**:411.
10. Engelman, D. M. 1972. *Chem. Phys. Lipids.* **8**:298.
11. Fischer, S., M. Cellino, F. Zambrano, G. Zampighi, M. Tellez Nagel, D. Marcus, and M. Canessa-Fischer. 1970. *Arch. Biochem. Biophys.* **138**:1.
12. Gemme, G. 1968. *Life Sci.* **7**:1239.
13. Hayashi, M., T. Muramatsu, and I. Hara. 1972. *Biochim. Biophys. Acta.* **255**:98.
14. Hicks, R. M., and B. Ketterer. 1969. *Nature (Lond.).* **224**:1304.
15. Hille, B. 1971. *J. Gen. Physiol.* **58**:599.
16. Hodgkin, A. L., and A. F. Huxley. 1952. *J. Physiol. (Lond.).* **117**:500.
17. Holtzman, E., A. R. Freeman, and L. A. Kashner. 1970. *J. Cell Biol.* **44**:438.
18. Keynes, R. D. 1972. *Nature (Lond.).* **239**:29.
19. Keynes, R. D., J. M. Ritchie, and E. Rojas. 1971. *J. Physiol. (Lond.)* **213**:235.
20. Loewenstein, W. R. 1966. *Ann. N. Y. Acad. Sci.* **137**:441.
21. McNutt, N. S., and R. S. Weinstein. 1973. *Prog. Biophys. Mol. Biol.* **26**:45.
22. Moore, J. W., T. Narahashi, and T. I. Shaw. 1967. *J. Physiol. (Lond.).* **188**:99.
23. Peracchia, C. 1973. *J. Cell Biol.* **57**:54.
24. Peracchia, C. 1973. *J. Cell Biol.* **57**:66.

25. PERACCHIA, C., and B. S. MITTLER. 1972. *J. Cell Biol.* **53**:234.
26. PERACCHIA, C., and J. D. ROBERTSON. 1971. *J. Cell Biol.* **51**:223.
27. PETERSON, R. P., and F. E. PEPE. 1961. *J. Biophys. Biochem. Cytol.* **11**:157.
28. PINTO DA SILVA, P. 1973. *Proc. Natl. Acad. Sci. U. S. A.* **70**:1339.
29. PINTO DA SILVA, P., and D. BRANTON. 1970. *J. Cell Biol.* **45**:598.
30. PINTO DA SILVA, P., S. D. DOUGLAS, and D. BRANTON. 1971. *Nature (Lond.).* **232**:194.
31. SABATINI, M., R. DIPOLO, and R. VILLEGAS. 1968. *J. Cell Biol.* **38**:176.
32. SATO, T. 1968. *J. Electron Microsc.* **17**:158.
33. SINGER, M., and M. R. GREEN. 1968. *J. Morphol.* **124**:321.
34. SINGER, M., and M. M. SALPETER. 1966. *J. Morphol.* **120**:281.
35. SMALL, D. M. 1967. *J. Lipid Res.* **8**:551.
36. STAEHELIN, L. A. 1972. *Proc. Natl. Acad. Sci. U. S. A.* **69**:1318.
37. STAEHELIN, L. A., F. J. CHLAPOWSKI, and M. A. BONNEVILLE. 1972. *J. Cell Biol.* **53**:73.
38. TILLACK, T. W., and V. T. MARCHESI. 1970. *J. Cell Biol.* **45**:649.
39. TILLACK, T. W., R. E. SCOTT, and V. T. MARCHESI. 1972. *J. Exp. Med.* **135**:1209.
40. VERGARA, J., W. LONGLEY, and J. D. ROBERTSON. 1969. *J. Mol. Biol.* **46**:593.
41. VILLEGAS, G. M. 1969. *J. Ultrastruct. Res.* **26**:501.
42. VILLEGAS, G. M. 1971. *Acta Cient. Venez.* **22** (Suppl. R6):2.
43. VILLEGAS, G. M., and R. VILLEGAS. 1968. *J. Gen. Physiol.* **51**(Suppl.):44s.
44. WISSIG, S. L., and D. O. GRANEY. 1968. *J. Cell Biol.* **39**:564.
45. ZAMBRANO, F., M. CELLINO, and M. CANESSA-FISCHER. 1971. *J. Membrane Biol.* **6**:289.